

Analysis of Automatic Rigid Image-Registration on Tomotherapy

- 토모테라피의 자동영상정합 분석 -

¹⁾Dept. of Radiation Oncology, College of Medicine, Soonchunhyang University of Korea ·

²⁾Dept. of Medical Information Technology Engineering, Soonchunhyang University of Korea ·

³⁾Dept. of Biomedical Engineering and Research Institute of Biomedical Engineering, College of Medicine, The Catholic University of Korea · ⁴⁾Dept. of Radiology, Shin-Gu University of Korea ·

Young-Lock Kim^{1, 2)} · Kwang Hwan Cho¹⁾ · Jae-Hong Jung^{1, 3)} · Joo-Young Jung³⁾ ·
Kwang Chae Lim^{1, 2)} · Yong Ho Kim¹⁾ · Seong Kwon Moon¹⁾ · Sun Hyun Bae¹⁾ ·
Chul Kee Min¹⁾ · Eun Seog Kim¹⁾ · Seung-Gu Yeo¹⁾ · Tae Suk Suh³⁾ ·
Bo-Young Choe³⁾ · Jung-Whan Min⁴⁾ · Jae Ouk Ahn²⁾

— Abstract —

The purpose of this study was to analyze translational and rotational adjustments during automatic rigid image-registration by using different control parameters for a total of five groups on TomoTherapy (Accuray Inc, Sunnyvale, CA, USA). We selected a total of 50 patients and classified them in five groups (brain, head-and-neck, lung, abdomen and pelvic) and used a total of 500 megavoltage computed tomography (MVCT) image sets for the analysis. From this we calculated the overall mean value(M) for systematic and random errors after applying the different control parameters. After randomization of the patients into the five groups, we found that the overall mean value varied according to three techniques and resolutions. The deviation for the lung, abdomen and pelvic groups was approximately greater than the deviation for the brain and head-and-neck groups in all adjustments. Overall, using a “full-image” produces smaller deviations in the rotational adjustments. We found that rotational adjustment has deviations with distinctly different control parameters. We concluded that using a combination of the “full-image” technique and “standard” resolution will be helpful in assisting with patients’ repositioning and in correcting for set-up errors prior to radiotherapy on TomoTherapy.

Key words : Tomotherapy, Image guided radiation therapy, Megavoltage computed tomography, Image-registration

I . INTRODUCTION

Intensity-modulated radiation therapy (IMRT) can

* 접수일(2013년 12월 30일), 1차 심사일(2014년 2월 10일), 2차 심사일(2014년 3월 4일), 확정일(2014년 3월 13일)

교신저자: 정재홍, (420-767) 경기도 부천시 원미구 조마루로 170
순천향대학교 의과대학 방사선종양학교실
Tel: 032-621-5784 Fax: 032-621-5885
E-mail : rtjung@catholic.ac.kr

optimize dose distribution in the tumor even as the prescription dose is increased as it is possible to derive a better dose-volume histogram (DVH) for complex anatomical structures or the surrounds of critical organs by using the multi-leaf collimators (MLCs)¹⁻³⁾. By using magnetic resonance imaging (MRI), positron emission tomography (PET) and other modalities which have the capability of

producing high-resolution images and the building of an image database through the development of medical imaging⁴⁾. However, the treatment uncertainties can arise during treatment because of weight loss in patients, decrease in tumor volume and patient set-up errors when high-precision IMRT techniques are required. Accurate patient positioning is a very important consideration in the pre-treatment process during a course of treatment. We can reduce patient set-up errors by using image-guided radiation therapy (IGRT), and improve the accuracy of delivery of radiation therapy with various techniques⁵⁻⁷⁾.

Tomotherapy (Accuray Inc, Sunnyvale, CA, USA) is a unique type of radiation therapy. The equipment combines a linear accelerator (LINAC) with computed tomography (CT). Spiral radiation therapy is achieved by the use of a gantry head with a 360° range of rotation and couch motion⁸⁾. IMRT with Tomotherapy can realized properly tumor prescribed dose optimization. In addition, image-registration using megavoltage computed tomography (MVCT) is useful for performing IGRT techniques^{9, 10)}. In MVCT scanning, a user can select two parameters: the slice-thickness (mm) mode and the scan length (mm). In general, the slice-thickness options are coarse (6 mm), normal (4 mm) and fine (2 mm) modes^{11, 12)}.

The image-registration is divided into two categories (manual and automatic), respectively. Different control parameters in automatic rigid image-registration can be selected to adjust for each fraction. The parameters are further divided depending on the density value (g/cm^3) and resolution (pixel)^{13, 14)}. We selected three types of density values: these are "bone", "bone-and-tissue" and "full-image". In the resolution algorithms, three algorithms are "standard", "fine" and "super-fine". We composed this method a total of nine different control parameters by using a combination of the three techniques and three algorithms. The type of possible displacements are translational (lateral, longitudinal and vertical) and rotational (pitch, roll

and yaw) directions^{9, 15-17)}. It is possible to correct roll errors, which is a rotational adjustment type of possible transformation parameter, by repositioning the gantry angle. Therefore, we compensated for errors through the process of image-registration. However, correction of the pitch and yaw displacements is impossible due to couch limitations in Tomotherapy. Patient repositioning is used for the correction of pitch and yaw errors during a course of treatment. In this study, we could confirm the results of previous analysis studies that looked at dose variation in relation to translational and rotational adjustments¹¹⁾.

In rigid image-registration process, accuracy in patient set-up and correcting for set-up errors are essential factors to ensure accuracy and reproducibility in radiation therapy. For example, Kaiser et al.¹⁸⁾ evaluated the rotational adjustments of the MVCT and kilovoltage computed tomography (kVCT) images of 15 head-and-neck and 20 prostate patients, respectively. Pitch deviations of the head-and-neck patients were smaller than those of the prostate patients, but the yaw angles were larger. Kaiser et al.¹⁸⁾ mentioned that although overall errors were small with respect to the rotational adjustments of the two groups, there should be consideration of small errors that may arise during a course of treatment. This study evaluated only two groups using the "bone" technique to verify the errors in the image-registration process. Schubert et al.¹⁹⁾ evaluated the translational and rotational adjustments of three groups: "the head-and-neck (N: 1,179), lung (N: 1,414), prostate (N: 1,274)". They verified the displacement values, in the image-registration process using the "bone" technique for the brain group and the "bone-and-tissue" technique for the other groups. Also, Schubert et al.¹⁹⁾ reported that daily-MVCT images could reduce patient set-up errors by better defining the anatomical structures for each treatment region. Therefore, the rigid image-registration of the MVCT is very important in Tomotherapy treatment.

The aim of this study was to analyze the impact

of different control parameter of the rigid image-registration on extend of translational and rotational adjustments in Tomotherapy. This study analyzed the automatic rigid image-registration of five groups of patients (brain, head-and-neck, lung, abdomen and pelvic patients).

II. MATERIALS AND METHODS

A. Patients and simulation

We selected a total of 50 patients who were divided into five groups (brain, head-and-neck, lung, abdomen and pelvic), and these patients were treated with Tomotherapy. Table 1 shows the data of the five groups in this study. A kVCT scanner (SOMATOM EMOTION, SIEMENS, Germany) and immobilization devices were used on all the patients. The brain and head-and-neck groups used thermoplastic mask (3-PT HEAD or 5-PT HEAD AND NECK SHOULDER, Orifit, Belgium) and the lung, abdomen and pelvic groups used BodyFix immobilization devices (Medical Intelligence, Elekta, Schwabmuchen, Germany) during the simulation. The reference points for the lead markers used during the radiation planning were the left, right and superior locations within a treatment region. For the acquisition of kVCT images for the brain and head-and-neck groups, the slice-thickness and resolution were 3 mm and 512 mm \times 512 mm, and

for the other groups, these values were 5 mm and 512 mm \times 512 mm. The kVCT images were exported to the pinnacle system (version 8.0, Philips Medical Systems, Andover, MA) and used for the contouring of the regions of interest (ROIs), the estimation of the gross tumor volume (GTV) and the identification of the organs at risks (OARs). This study used the Tomotherapy Hi-Art II treatment planning system (Accuray Inc, Sunnyvale, CA, USA).

B. MVCT scanning and image-registration process

For patient positioning during treatment, immobilization devices at simulation were equally applied and a movable red laser was used during the treatment. We acquired MVCT images by using mainly the coarse mode for all patients. The scan lengths (mm) included the length of the entire tumor volume for each group of different anatomical sites. All patients were scanned in order to obtain MVCT images for each fraction before treatment. For each of the fractions, we compared the acquired MVCT images and planning kVCT images during the process of automatic rigid image-registration. Figure 1, shows the registration process for head-and-neck patients. We applied the different density values ("bone": larger than 1.1 g/cm³, "bone-and-tissue": 0.3-1.1 g/cm³, and "full-image": all voxels) and resolutions ("standard": 128 \times 128, "fine": 256 \times 256, and "super-fine": 512 \times 512 matrix sizes)⁹.

Table 1. Patient characteristics of the five groups in this study.

Parameters	Treatment Site				
	Brain	H&N	Lung	Abdomen	Pelvic
Patients Number	10	10	10	10	10
Average age	62	62	59	61	57
Sex (M/F)	5/5	8/2	5/5	5/5	5/5
Fractions	10	10	10	10	10

Note: M = male; F = female; H&N = head-and-neck,

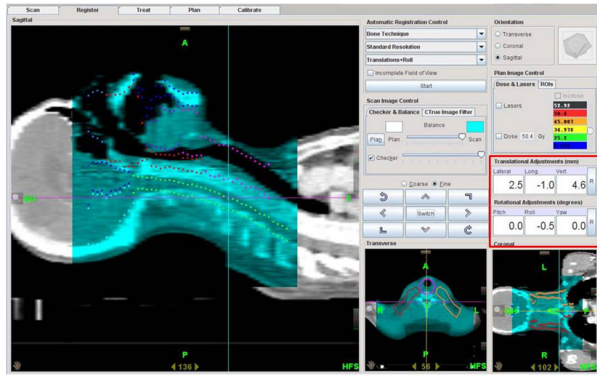


Fig. 1. View of the Tomotherapy operation station to check for translational and rotational set-up errors. Left figure shows the KVCT (gray color) and MVCT (green color) in a head-and-neck patient. Boundary red box shows set-up errors for this patient.

C. Data correction and analysis

In this study, we collected the displacement data of the translational (lateral, longitudinal and vertical) magnitudes (mm) and the rotational (pitch, roll and yaw) angles (°) of nine cases of automatic rigid image-registration processes for all patients, and we calculated the systematic and random errors for each of the groups^{20, 21)}.

First, we calculated the systematic error for each patient, with calculation of the mean of the inter-fractional variations for each fraction during a course of treatment. The displacements of two adjustments for all patient and groups were calculated using the following equations (1) and (2).

$$\begin{aligned} \text{Translational adjustment (mm)} = & \frac{\sqrt{(\text{Lateral})^2 + (\text{Longitudinal})^2 + (\text{Vertical})^2}}{\dots\dots\dots} \quad (1) \end{aligned}$$

$$\begin{aligned} \text{Rotational adjustment (angle)} = & \frac{\sqrt{(\text{Pitch})^2 + (\text{Roll})^2 + (\text{Yaw})^2}}{\dots\dots\dots} \quad (2) \end{aligned}$$

To calculate the systematic error mean value M

(μ_i) and the standard deviation $\Sigma(\mu_i)$ for all patients and groups, the following equation (3) was used.

$$\Sigma(\mu_i) = \sqrt{\frac{\sum_{i=1}^N (\mu_i - M(\mu_i))^2}{(N-1)}} \dots\dots\dots (3)$$

In this equation, μ_i is the systematic error for each patient (i), $M(\mu_i)$ is the systematic error mean value and N is the number of patients for each group in this study. For different image-registration components and between each group, statistical analysis was performed using a one-way ANOVA (analysis of variance).

Second, we calculated the random error for each patient, with calculation of the mean of the intra-fractional variations for each fraction during a course of treatment. For random errors of each patient per group, $\Sigma(\mu_R)$ is the standard deviation of the translational and rotational adjustments. Furthermore, we used the root-mean-square (RMS) to calculate the deviations between the five groups (Eq. 4). Finally, we calculated the overall mean value (M), using the standard deviation and RMS, to verify the overall deviations for the five groups (Eq. 5). The overall registration process of data collection and analysis are shown in Fig. 2.

$$\begin{aligned} RMS(\Sigma(\mu_R)) = & \sqrt{\sum_{i=1}^N \frac{(\Sigma(\mu_R))}{(N-1)}} \\ \text{where } \Sigma(\mu_R) = & \sqrt{\frac{\sum_{i=1}^N (\mu_R - M(\mu_R))^2}{(N-1)}} \quad \dots\dots\dots (4) \end{aligned}$$

$$\Sigma_{\text{Overall}}(M) = \sqrt{\Sigma(\mu_i)^2 + RMS(\Sigma(\mu_R))^2} \quad \dots\dots (5)$$

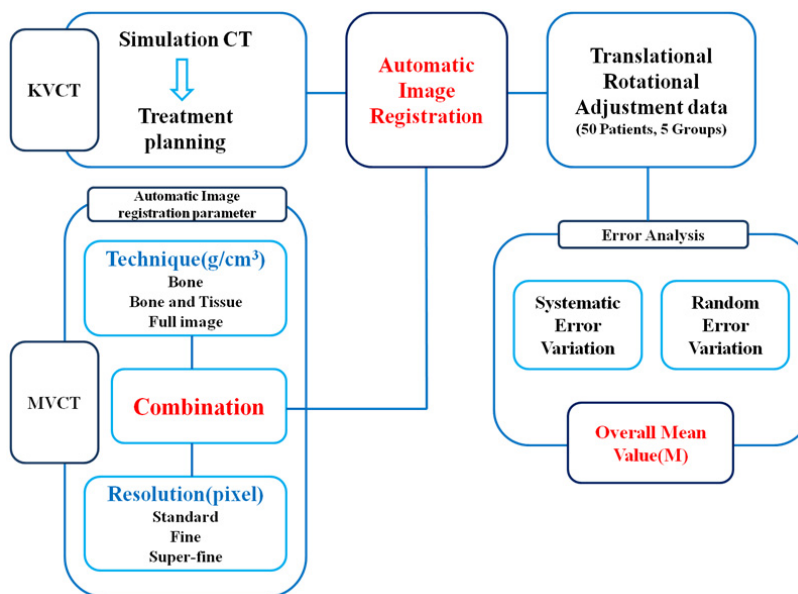


Fig. 2. View of the overall automatic rigid image-registration process of data collection and analysis.

Here, μ_R is the displacement of the random errors, $M(\mu_R)$ is the average of the displacements from the patients and $\Sigma(\mu_R)$ are the random errors for each of the groups.

In addition, we also analyzed the coefficient of correlation between the translational and rotational adjustments by using Pearson's product-moment coefficient to verify the correlations.

III. RESULTS AND DISCUSSION

In this study, we analyzed the deviations of the systematic errors and the RMS of random errors, and the overall mean value (M) by using the different control parameters, and dividing the patients into five groups. First, we found the differences in systematic errors $\Sigma(\mu_i)$ for two adjustments between each group. The brain and head-neck groups had smaller translational adjustments than the other groups. The brain group was 1.15 mm in the combination of "full-image and fine". The head-and-neck group was 1.36 mm in the combination of "full-image and super-fine". We

checked the equivalence of dispersion among the five groups. No significance on translational adjustment about the nine combinations shown in Table 2.

The rotational adjustment deviation with the "full-image" was mostly small. The rotational deviation of the pelvic group was 0.24° in the combination of "full-image and fine". Also, the results of the brain, head-and-neck, lung, and abdomen groups were 0.24° , 0.16° , 0.29° and 0.40° respectively in the combination of "full-image and super-fine". Kaiser et al.¹⁸⁾ evaluated the rotational adjustment variations in head-and-neck and prostate treatment. The results by using the "bone" technique showed that the deviations of head-and-neck patients were 1.19° , 1.53° and 1.42° for pitch, roll and yaw, respectively. Kaiser et al.¹⁸⁾ used MVCT images with resolution of 256×256 pixels, but we used MVCT images of 515×512 pixels. The statistical significance was confirmed by one-way ANOVA based on the combination of "full-image" and "standard" (Table 3). In the analysis of rotational adjustments, there is a significant difference of compared to "Bone technique" groups. The RMS value means the possible errors for a course of treatment fraction. The RMS of the random errors was analyzed for two

Table 2. Average and standard deviation of systematic errors (σ) for the translational directions (mm) between different image-registration components of the five groups.

Density (g/cm ³)	Resolution (pixel)	Treatment Site				
		Brain (mm)	H&N (mm)	Lung (mm)	Abdomen (mm)	Pelvic (mm)
Bone	Standard	4.04±1.82	5.88±1.82	7.46±4.58	8.56±3.53	7.27±3.94
	Fine	4.04±1.78	5.93±1.89	7.43±4.57	8.44±3.39	7.32±3.59
	Superfine	3.99±1.81	5.86±1.88	7.46±4.53	8.48±3.37	7.28±4.00
Bone & Tissue	Standard	3.98±1.81	5.75±1.87	7.62±4.79	8.73±3.80	7.50±3.89
	Fine	3.96±1.81	5.69±1.83	7.51±4.72	8.86±3.86	7.32±3.87
	Superfine	3.98±1.82	5.68±1.74	7.46±4.73	8.79±3.86	7.28±3.87
Full image	Standard	3.75±1.69	5.61±1.65	7.35±5.04	8.76±3.84	7.65±4.12
	Fine	3.74±1.61	5.52±1.54	7.37±4.93	8.76±3.75	7.59±3.97
	Superfine	3.73±1.60	5.51±1.54	7.37±4.83	8.66±3.90	7.50±4.00
p value		0.802	0.627	1.000	0.996	0.997

Table 3. Average and standard deviation of systematic errors (σ) for the rotational angles (°) between different image-registration components of the five groups (one-way ANOVA).

Density (g/cm ³)	Resolution (pixel)	Treatment Site				
		Brain (°)	H&N (°)	Lung (°)	Abdomen (°)	Pelvic (°)
Bone	Standard	1.62±1.04	0.91±0.52	1.46±0.89	0.96±0.77	1.41±1.02
	Fine	1.65±1.05	0.91±0.56	1.49±0.87	1.00±0.77	1.49±1.06
	Superfine	1.69±1.07	0.95±0.55	1.48±0.86	0.98±0.72	1.54±1.14
Bone & Tissue	Standard	0.75±0.73	0.62±0.39	0.79±0.62	0.49±0.59	0.85±0.74
	Fine	0.85±0.81	0.63±0.39	0.93±0.63	0.59±0.61	1.02±0.80
	Superfine	0.89±0.77	0.66±0.35	0.97±0.63	0.62±0.62	1.01±0.78
Full image	Standard	0.44±0.41	0.49±0.34	0.66±0.58	0.38±0.52	0.47±0.41
	Fine	0.56±0.49	0.51±0.30	0.70±0.54	0.47±0.56	0.48±0.45
	Superfine	0.59±0.45	0.51±0.29	0.74±0.50	0.52±0.55	0.52±0.46
p value		p < 0.01				

adjustments for each group. In this study, the RMS value in translational adjustments was 1.12 mm for the brain group with the combination of "full-image and super-fine". The head-and-neck group was 0.80 mm in the combination of "full-image and fine". The lung, abdomen and pelvic groups were small with the combination "bone and super-fine", "full-image and standard" and "full-image and fine", individually. For rotational adjustments, the brain, abdomen and pelvic groups were 0.33°,

0.32° and 0.32° in the combination of "full-image and standard", respectively. The head-and-neck and lung groups were 0.24° and 0.41° in the combination of "full-image and super-fine", respectively. Lee et al.²²⁾ evaluated the accuracy for the different combinations of automatic registration selection factors for a total of 5 patients (2 cranial and 3 external cranial cases). They reported that the combination of "full-image and super-fine" was the best option in the cranial cases. Also, the combi-

nations, both "bone and super-fine", and "full-image and super-fine", were the best in external cranial cases. Their results were similar with the results in our study. Using the "full-image" has mainly less the variations in rotational adjustments in our study. Furthermore, we evaluated the data from the five groups more extensively compared to their study. We found differences between two factors, namely those related to anatomical sites and the correlation of translational and rotational adjustment in the image-registration process. As a result, we have to confirm various anatomical regions due to the variation of the errors that may arise depending on the different control parameters during the automatic rigid image-registration process.

Table 4 shows the results of the overall mean (M) for the two adjustments performed for each group. In the translational adjustments, the brain

and head-and-neck groups were 1.63 mm and 1.59 mm in the combination of "full-image and super-fine". For the rotational adjustments, all groups were mostly small in "full-image" technique. The head-and-neck and lung groups were relatively small at 0.29° and 0.50° in the combination of "full-image and super-fine", respectively. Also, the brain, abdomen and pelvic groups were 0.41° , 0.53° and 0.41° in the combinations of "full-image and standard", respectively. Figs. 3 and 4 show the magnitude of each of the translational and rotational adjustments. In this study, the overall mean value (M) differed according to the three techniques and three resolutions. In most cases, the deviations of the lung, abdomen and pelvic groups were greater than those of the brain and head-and-neck groups in all adjustments. For this part, Schubert et al.¹⁹⁾ analyzed three parameters (3D vector translational shifts) and roll rotations for brain and head-

Table 4. Overall (M) of translational directions (mm) and rotational angles ($^\circ$) between different image-registration components of the five groups.

Directions	Density (g/cm ³)	Resolution (pixel)	Treatment Site					
			Brain	H&N	Lung	Abdomen	Pelvic	
Translation (mm)	Bone	Standard	1.86	1.87	4.68	3.55	4.01	
		Fine	1.82	1.91	4.67	3.48	4.03	
		Superfine	1.85	1.92	4.62	3.44	4.08	
	Bone & Tissue	Standard	1.85	1.93	4.91	3.90	3.95	
		Fine	1.85	1.89	4.83	3.97	3.93	
		Superfine	1.87	1.80	4.83	3.97	3.94	
	Full image	Standard	1.72	1.70	5.16	3.95	4.21	
		Fine	1.64	1.59	5.05	3.85	4.06	
		Superfine	1.63	1.59	4.95	4.10	4.09	
	Rotation ($^\circ$)	Bone	Standard	1.04	0.52	0.91	0.78	1.04
			Fine	1.06	0.56	0.89	0.78	1.17
			Superfine	1.08	0.55	0.88	0.74	1.17
Bone & Tissue		Standard	0.74	0.40	0.63	0.60	0.76	
		Fine	0.82	0.40	0.64	0.62	0.82	
		Superfine	0.77	0.36	0.64	0.63	0.80	
Full image		Standard	0.41	0.34	0.59	0.53	0.41	
		Fine	0.49	0.30	0.54	0.57	0.45	
		Superfine	0.45	0.29	0.50	0.56	0.46	

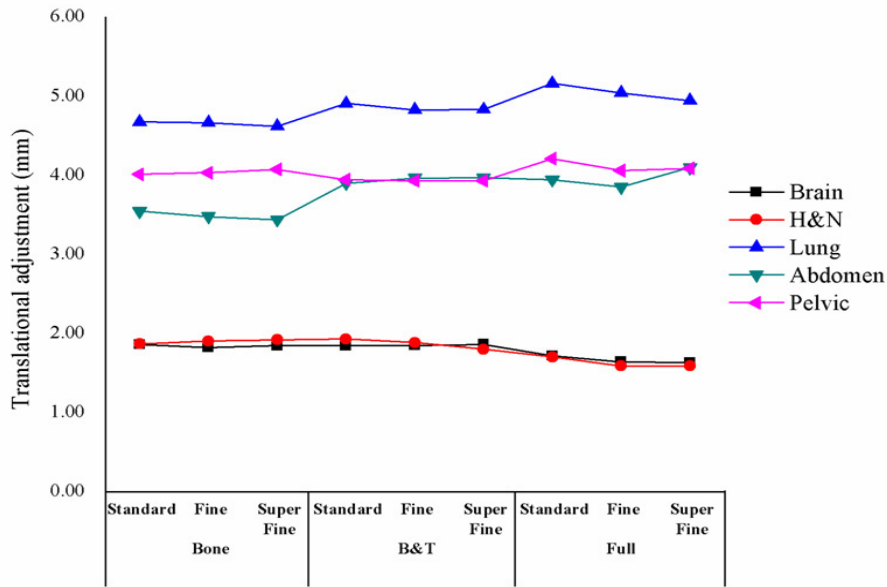


Fig. 3. Overall mean values (M) of translational directions (mm) between different image-registration components of the five groups.

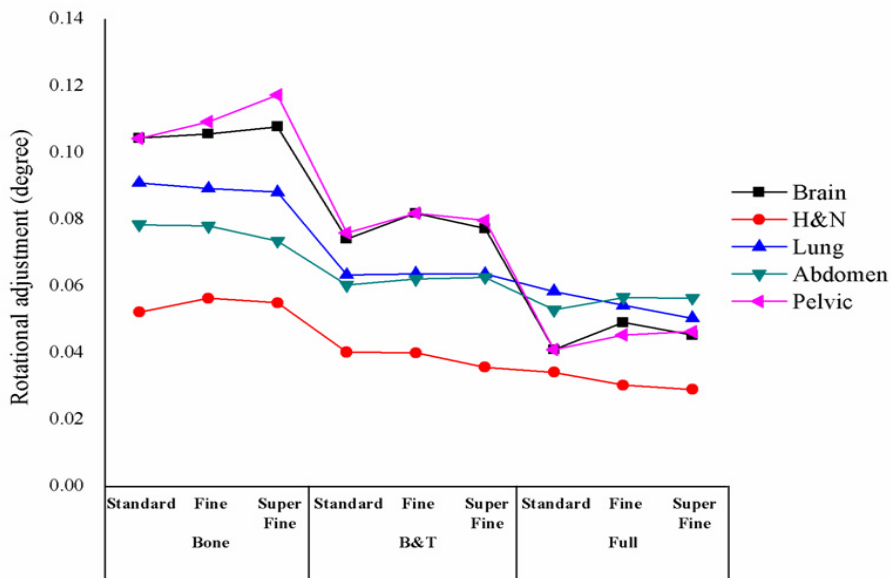


Fig. 4. Overall mean values (M) of rotational angles ($^{\circ}$) between different image-registration components of the five groups.

and-neck, and lung. And they reported that deviations of set-up errors were observed among the various groups. Their results showed that systematic error variations and random error magnitudes ranged from 1.6 mm-2.6 mm for both brain and head-and-neck groups. For the lung and prostate groups, the range was 3.2 mm-7.2 mm. For the roll rotations, the brain, head-and-neck groups

were 0.8° - 1.2° , while the lung and prostate groups were 0.5° - 1.0° . For these measurements, they did not analyze pitch and yaw angles in rotational adjustments. By comparison, we performed the analysis by examining a total of 50 patients divided into five groups which were the brain, head-and-neck, lung, abdomen and pelvic groups. We also analyzed the displacement data for the

translational (lateral, longitudinal and vertical) and the rotational (pitch, roll and yaw) adjustments. For accuracy of automatic image-registration using a phantom, Boswell et al.¹¹⁾ acquired 104 MVCT scans from an anthropomorphic head phantom. Moreover, they calculated the translational displacements from the planning image set, in a division of 18 combinations. The head phantom study compared the automatic image-registration to the optical tracking and manual method. The experimental uncertainty was approximately within 1 mm. The phantom test showed the results from precise data, and various studies have followed those results. We did not check the verification of the phantom, and we assessed the MVCT automatic image-registration for translational and rotational adjustments without phantom experiments.

The Tomotherapy software has been updated periodically, but there is the limitation of time in the automatic rigid image-registration process. In general, registration process time ranges is from 8 seconds to more than 1 minute. The process time of obtaining "super-fine" resolution takes more time than for the other resolutions^{11, 13)}. We also calculated the overall mean value (M) variations related to resolution for all groups. In this calculation, 66.7% of the translational variation was less than 0.05 mm (range: 0.01-0.12 mm) and 93.7% of the rotational variations were less than 0.05° ($0.00-0.07^\circ$) (Table 4). The variation was small due to the resolution.

Additional study was performed for the correlation coefficient values for two adjustments for each group. The correlation between the vertical and pitch directions showed significant differences (-0.667 , $p < 0.05$) in the brain group. The head-and-neck group was significantly different with a value of 0.702 ($p < 0.05$) for both the lateral directions and roll angles and the longitudinal directions and yaw angles (-0.646 , $p < 0.05$). Furthermore, the lung group showed significant differences in the lateral and longitudinal directions (0.702 , $p < 0.05$), lateral directions and roll angles

(-0.787 , $p < 0.01$) and longitudinal directions and pitch angles (0.665 , $p < 0.05$). In the abdomen group, the yaw and roll angles were significantly different -0.847 ($p < 0.01$). However, there were no significant differences in the pelvic group for all directions and rotations.

IV. CONCLUSIONS

In this study, we analyzed by examining a total of 50 patients divided into five groups which were the brain, head-and-neck, lung, abdomen and pelvic regions. The rotational adjustments have varying deviations depending on different control parameters, and also the variations between the different resolutions were small. Therefore, using a combination of the "full-image" technique and "standard" resolution will be helpful in assisting patients' repositioning, and in correcting for set-up errors prior to radiotherapy with Tomotherapy.

REFERENCES

1. Ezzell GA, Galvin JM, Low D, et al. Guidance document on delivery, treatment planning, and clinical implementation of IMRT: report of the IMRT Subcommittee of the AAPM Radiation Therapy Committee, *Med Phys*, 30(8), 2089-2115, 2003
2. Vergeer MR, Doornaert PA, Rietveld DH, Leemans CR, Slotman BJ, Langendijk JA. Intensity-modulated radiotherapy reduces radiation-induced morbidity and improves health-related quality of life: results of a non-randomized prospective study using a standardized follow-up program, *Int J Radiat Oncol Biol Phys*, 74(1), 1-8, 2009
3. Bucci MK, Bevan A, Roach M 3rd. Advances in radiation therapy: conventional to 3D, to IMRT, to 4D, and beyond, *CA Cancer J Clin*, 55(2), 117-134, 2005

4. Aird EG, Conway J. CT simulation for radiotherapy treatment planning, *Br J Radiol*, 75(900), 937-949, 2002
5. Yartsev S, Kron T, Van Dyk J. Tomotherapy as a tool in image-guided radiation therapy (IGRT): theoretical and technological aspects, *Biomed Imaging Interv J*, 3(1), e16, 2007
6. Yartsev S, Kron T, Van Dyk J. Tomotherapy as a tool in image-guided radiation therapy (IGRT): current clinical experience and outcomes, *Biomed Imaging Interv J*, 3(1), e17, 2007
7. Mackie TR, Kapatoes J, Ruchala K, et al. Image guidance for precise conformal radiotherapy, *Int J Radiat Oncol Biol Phys*, 56(1), 89-105, 2003.
8. Mackie TR, Holmes T, Swerdloff S, et al. Tomotherapy: a new concept for the delivery of dynamic conformal radiotherapy, *Med Phys*, 20(6), 1709-1719, 1993
9. Woodford C, Yartsev S, Van Dyk J. Optimization of megavoltage CT scan registration settings for brain cancer treatments on tomotherapy, *Phys Med Biol*, 52(8), 185-193, 2007
10. James SW. Helical tomotherapy in the community setting: a personal account, *Commun Oncol*, 6(10), 463-467, 2009
11. Boswell S, Tomé W, Jeraj R, Jaradat H, Mackie TR. Automatic registration of megavoltage to kilovoltage CT images in helical tomotherapy: an evaluation of the setup verification process for the special case of a rigid head phantom, *Med Phys*, 33(11), 4395-4404, 2006
12. Shah AP, Langen KM, Ruchala KJ, Cox A, Kupelian PA, Meeks SL. Patient dose from megavoltage computed tomography imaging, *Int J Radiat Oncol Biol Phys*, 70(5), 1579-1587, 2008
13. Ruchala KJ, Olivera GH, and Kapatoes JM. Limited-data image registration for radiotherapy positioning and verification, *Int J Radiat Oncol Biol Phys*, 54(2), 592-605, 2002
14. Meeks SL, Harmon JF Jr, Langen KM, Willoughby TR, Wagner TH, Kupelian PA. Performance characterization of megavoltage computed tomography imaging on a helical tomotherapy unit, *Med Phys*, 32(8), 2673-2681, 2005
15. Mahan SL, Ramsey CR, Scaperoth DD, Chase DJ, Byrne TE. Evaluation of image-guided helical tomotherapy for the retreatment of spinal metastasis, *Int J Radiat Oncol Biol Phys*, 63(5), 1576-1583, 2005
16. Zeidan OA, Langen KM, Meeks SL, et al. Evaluation of image-guidance protocols in the treatment of head and neck cancers, *Int J Radiat Oncol Biol Phys*, 67(3), 670-677, 2007.
17. Liu H, Wu Q. Evaluations of an adaptive planning technique incorporating dose feedback in image-guided radiotherapy of prostate cancer, *Med Phys*, 38(12), 6362-6370, 2011
18. Kaiser A, Schultheiss TE, Wong JY, et al. Pitch, roll, and yaw variations in patient positioning, *Int J Radiat Oncol Biol Phys*, 66(3), 949-955, 2006
19. Schubert LK, Westerly DC, Tomé WA, et al. A Comprehensive assessment by tumor Site of patient setup using daily MVCT imaging from over three 3,800 helical tomotherapy treatments, *Int J Radiat Oncol Biol Phys*, 73(4), 1260-1269, 2009
20. Yan D, Wong J, Vicini F, et al. Adaptive modification of treatment planning to minimize the deleterious effects of treatment setup errors, *Int J Radiat Oncol Biol Phys*, 38(1), 197-206, 1997
21. Yan D, Lockman D, Martinez A, et al. Computed tomography guided management of interfractional patient variation, *Semin Radiat Oncol*, 15(3), 168-179, 2005
22. Lee S, Cao YJ, Shim JB, et al. Evaluation of the Accuracy of Different Combinations of Automatic Registration Selection Factors in Obtaining Tomotherapy Megavoltage Computed Tomography Images, *J Korean Phys Soc*, 60(11), 1961-1966, 2012

토모테라피의 자동영상정합 분석

김영록^{1, 2)} · 조광환¹⁾ · 정재홍^{1, 3)} · 정주영³⁾ · 임광채^{1, 2)} · 김용호¹⁾ · 문성권¹⁾ · 배선현¹⁾ · 민철기¹⁾ · 김은석¹⁾ ·
여승구¹⁾ · 서태석³⁾ · 최보영³⁾ · 민정환⁴⁾ · 안재억²⁾

¹⁾순천향대학교 의과대학 방사선종양학교실 · ²⁾순천향대학교 산업정보대학원 의료공학과 ·
³⁾가톨릭대학교 의과대학 의공학교실, 생체의공학연구소 · ⁴⁾신구대학교 방사선과

본 연구는 토모테라피(Accuray Inc, Sunnyvale, CA, USA)의 자동영상정합 과정에서 조정인자에 따른 종축과 회전축의 오차를 분석하였다. 다섯그룹(두부, 경부, 흉부, 복부, 골반부)으로 구분된 총 50명의 치료가 종료된 환자를 대상으로 하였고, 총 500개의 megavoltage computed tomography (MVCT) 영상을 분석하였다. 모의치료에서 kilovoltage computed tomography (kVCT)영상을 얻었고, 치료계획을 위하여 토모테라피 Hi-Art II 치료계획시스템(Accuray Inc, Sunnyvale, CA, USA)을 사용하였다. 매 회 치료 전 자동영상정합 과정을 시행하였고, 종축과 회전축의 오차를 기록하였다. 종축과 회전축의 일치도(adjustments)에서 자동영상정합을 분석하기 위하여 총 이홉 가지 조정인자를 적용하였고, 각 그룹의 계통적(systematic, Σ)과 통계적(random, RMS) 오차에 대하여 종합적 평균오차(overall mean value, M)를 구했다. 각 그룹 간 회전축 일치도의 종합적 평균오차에서 밀도와 해상도에 따른 다양한 조정인자에 의한 차이를 보였다. 밀도와 해상도가 높아짐에 따라 회전축 일치도에서 편차가 작았다. 그러므로, 토모테라피에서 "full-image"모드와 "standard"해상도를 이용한 자동영상정합은 정확한 오차 확인이 가능하고, 환자 재위치잡이(repositioning) 및 보정(correcting)에 도움이 될 것으로 사료된다.

중심단어: 토모테라피, 영상유도방사선치료, 고에너지 전산화단층촬영, 자동영상정합